Available online at www.sciencedirect.com
SCIENCE DIRECT®
PERGAMON
International Journal of Multiphase Flow 29 (2003) 1137–1152
International Journal of Multiphase Flow
www.elsevier.com/locate/ijmulflow

Heterogeneous condensation process in an air water vapour expansion through a nozzle—experimental aspect

K. Jurski [a], E. Géhin [b,*]

[a] *Laboratoire de Biorhéologie et d'Hydrodynamique Physicochimique, L.B.H.P. ESA CNRS 7057, Université Paris VII, 2 place jussieu, 75251 Paris Cedex, France*
[b] *CERTES, Université Paris XII, Avenue du Général de Gaulle, 94010 Créteil Cedex, France*

Received 1 November 2001; received in revised form 13 April 2003

Abstract

This paper describes an experimental study of heterogeneous condensational growth process with limited vapour source in a turbulent flow in a nozzle. The nature, diameter and concentration of the seeding particles are known and controlled. We measure the velocity and diameter of droplets at different positions in the converging part of the nozzle. The experimental results present the diameter evolution of the water coated seeding particles.

Keywords: Heterogeneous condensational; Growth rate; Turbulent flow; Nozzle; Seeding particles; Air water vapour expansion; Aerodynamic diameter; Saturation

1. Introduction

Many industrial processes in nuclear, thermal and chemical engineering are concerned with two-phase flows in different configurations. In order to define the containment load conceptions or to evaluate the consequences of fluid release to the environment, direct experimental investigations on how the gas–liquid configuration develops during the slit passage is often not available. In these cases, modelling can help investigate the discharge of a gas–liquid mixture with the aim to comply with the safety requirements. One can notice an unavoidable trend to use more elaborate physical models which involve simulations of complex flows and mass–heat transfer processes in

* Corresponding author.
E-mail addresses: jurski@ccr.jussieu.fr (K. Jurski), gehin@univ-paris12.fr (E. Géhin).

0301-9322/03/$ - see front matter
doi:10.1016/S0301-9322(03)00083-1

fluids with several phases and/or components. The quality of this predictive models strongly depends on the understanding of the physical phenomena governing these flows.

Pipes or reservoirs at high pressure conditions normally contain single-phase fluids (vapour, dry air and vapour mixture). When a crack accidentally occurs, vigorous depressurisation begins with sonic flow of annular and/or dispersed two-phase type through the slit (Selmer Olsen, 1991; Lemonnier and Camelo Cavalcanti, 1993). In order to characterize flow of such a gas–liquid mixture, the knowledge of inter-phase interactions and transfer mechanisms during the slit passage is required. This necessitates to identify the dominant parameters that affect the condensation process. Because vapour flows are often mixed with impurities, we need to examine to what extent these aerosols affect the condensation activation process, the size and concentration of the generated droplets.

One finds many theoretical studies of the droplet growth by vapour condensation in nozzle because many industrial processes involve this type of flow (Turner et al., 1988; Tom and Debenedetti, 1991; Johnston and Wexler, 1995; Mallina and Wexler, 1997; Yang et al., 2000; Bayazitoglu et al., 1996; Williams, 1996). However, experimental studies of droplet growth by heterogeneous condensation process in turbulent flows are limited because of the difficulties in measuring the final and initial droplet sizes and concentrations. Vatazhin et al. (1995) measured the size and concentration of droplets formed by heterogeneous condensation of vapour on cigarette smoke flowing through a nozzle. However, in this experimental study, the initial characteristics of the nuclei is unknown. Some experimental studies are also concerned with homogeneous vapour condensation in nozzles (Wenqing and Jinfan, 1995; Lesniewski and Friedlander, 1997; Young, 1982). The results of these works cannot be used for determination of the growth rate of droplets because the initial nuclei concentration and the nucleation rate cannot be easily determined. Some other authors studied heterogeneous condensation in laminar flows. In these studies the droplets' physical parameters are determined and their results confirm the theoretical physical models available (Rebours et al., 1996; Kulmala et al., 1995; Hughmark, 1967). All these studies are a starting point for the present study. Unfortunately, they do not investigate the influence on the vapour-droplets mass transfer of the instantaneous mechanical non-equilibrium between phases caused by turbulent fluctuations. Vatazhin et al. (1995) underlined that droplets growing by heterogeneous condensation do not correctly follow the turbulent flow and suggested therefore that this process influences the mass transfer between the vapour and the droplets.

In this paper we study heterogeneous condensational growth with limited vapour source in a turbulent flow.

2. Droplet diameter evolution by heterogeneous condensation process in a nozzle

2.1. Activation

When an aerosol is initially present in a gas carrier phase combined with vapour, Wilson (1927) observed that condensation is reached at low saturation conditions: heterogeneous condensation can occur at saturation ratio a few percents greater than saturation. The vapour molecules deposit on the aerosol surface because of the sticking forces. The liquid film thus formed on the aerosol has a large curvature radius (compared to molecular dimensions) promoting deposition of vapour molecules according to the Kelvin effect.

Hinds (1982) defined two kinds of aerosol: soluble and insoluble nuclei. Condensation mechanism on soluble and insoluble nuclei are still the subject of research (Gorbunov and Hamilton, 1997; Sachweh et al., 1996; Cruz and Pandis, 1996). Among the insoluble particles, Reist (1984) identified roughly the "wettable" and "non-wettable" nuclei. During the growth by vapour condensation, wettable nuclei look like droplets. In most cases, these droplets are considered as pure liquid droplets. When the nucleus is not wettable, the vapour tends to deposit in the form of very small droplets on its surface. When the nucleus surface is completely covered, a uniform liquid film appears, the nucleus is then entirely coated. Fletcher (1962) theoretically treated this phenomenon by considering the contact angle between the nucleus and small liquid droplets formed on its surface. These studies confirmed experimental observations showing large saturation ratios were required for a non-wettable nucleus to be activated by vapour condensation.

If an insoluble nucleus needs large saturation ratios for condensational growth, a soluble nucleus can serve as a condensation nucleus at low saturation and even subsaturation conditions (Friedlander, 1977; Reist, 1984). When soluble and insoluble nuclei are present together in a medium with saturation greater than 1, one can easily understand that soluble nuclei first initiate the condensational growth.

2.2. Droplets growth

The growth rate of droplets by condensation of water vapour and heat release are usually expressed by Mason's equations (Mason, 1971) for continuum regime. These equations can be corrected for non-continuum effect using the Knudsen factor (Loyalka and Park, 1988). Furthermore, Mason's equations were derived from static conditions for a particle without relative motion in the surrounding gas. If the surrounding gas moves with respect to the particle, the exchange rate is increased. The mass and heat transfer rate is then corrected by introducing the Sherwood and Nusselt numbers (Bird et al., 1960; Williams and Loyalka, 1991).

3. Saturation methods

Saturation rate greater than 1 and therefore condensation can result from different physical processes, all of them consisting in cooling the mixture vapour–inert gas, as for example:

- adiabatic expansion in a Wilson-type cloud chamber or in a converging–diverging nozzle,
- hot gas carrying a condensable vapour mixed with a cool gas,
- radiative or conductive cooling.

The adiabatic expansion of sheath air through a nozzle can reach a saturation ratio approaching one hundred (Papon and Leblond, 1990). Because this method leads to high values of S, a lot of experimental and theoretical studies have been performed for understanding and predicting homogeneous condensation in supersonic nozzles.

Using an inert gas–vapour mixture exempt from any impurities, the homogeneous condensation mechanism takes place at high saturation ratios in the diverging part of the nozzle (supersonic zone) on vapour molecules aggregates. This fog formation is accompanied by the release of

the latent heat of vaporisation of the condensate. The local pressure rise thus induced has been termed "condensation shock" (Hidy, 1984; Wegener and Pouring, 1964; Wegener, 1969; Turner et al., 1988).

In a typical experiment with air, when vapour and impurities expand through a nozzle, both pressure and temperature drop, and saturation conditions for condensation may be reached at the subsonic section upstream the throat. This condensation mode, which starts on existing particles at saturation ratios near unity, does not involve a condensation shock.

In order to develop a new class of instruments based on the physical and chemical characterisation of particles subjected to a strong rapid acceleration field in a nozzle, Johnston and Wexler (1995), Mallina and Wexler (1997) analyse the heterogeneous condensation process for different shapes of the converging nozzle. They pointed out that the condensational growth in the nozzle strongly depends upon the converging zone length and underlined that droplet growth was reduced in the case of "a short" converging nozzle.

4. Characterisation of a wet air—monodisperse aerosol mixture flow through a nozzle

Here we analyse the flow of wet air and impurities induced by an accidental crack in a pipe or reservoir with high pressure conditions. The experiments consist in initiating the water droplets formation in a wet air seeded with a monodispersed di-octyl-phtalate (DOP) aerosol with known concentration and diameter.

4.1. Experimental setup

Experimental requirements linked with dispersed two-phase flow through a slit have lead to several instrumental installations. In order to accurately simulate the dispersed two-phase flow behaviour through a slit, several criteria must be respected:

- a converging–diverging nozzle as an ideal simulation of leak through cracks (Lemonnier and Camelo Cavalcanti 1993),
- a homogeneous repartition of the dispersed phase in the continuous phase at the entrance of the nozzle,
- non-intrusive instrumentation,
- a short nozzle geometry with a circular section (Amos and Schrock, 1984) or a rectangular one (Chexal et al., 1984; Chexal and Horowitz, 1987).

4.1.1. Flow loop

The experimental installation consists of a flow loop capable to produce dispersed flows rapidly accelerated in a converging–diverging nozzle. Experiments are performed under ambient temperature conditions with initial downstream pressure conditions lower than 10^6 Pa. The dispersed condensed phase is obtained by spontaneous vapour condensation on DOP nuclei already present in the upstream reservoir. Thereby, when the discharge starts, nuclei are carried away and dispersed in the continuum of the gas phase. Gas and DOP nuclei enter the nozzle as a homogeneous

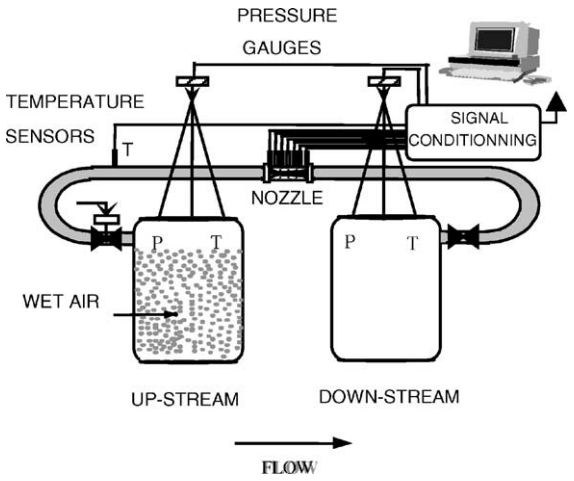

Fig. 1. Schematic representation of the flow loop.

mixture. This type of configuration represents a good approach in the study of accidental flow of gas—droplet mixture through a slit.

The flow loop (Fig. 1) consists of two identical reservoirs connected with a duct including a converging–diverging nozzle (Jurski, 1997):

- each reservoir volume is 0.86 m^3,
- the flow duct (diameter 82 mm) is equipped with a pneumatic winnow to start the discharge through the nozzle,
- the nozzle (Fig. 2), with a rectangular section, is made of two transparent Pyrex walls (30 mm thick each) which offer an optical access to the flow. Its dimensions and the ratio to the section at the position z to the throat section (A_z/A_{th}) are given in Tables 1 and 2.

The flow loop is instrumented in order to measure pressure, temperature, mass flow rate and droplet velocities in the nozzle:

- Pressure is measured by nine gauge sensors: one in each reservoir and seven along the nozzle.
- Temperature is measured by five K type thermocouples. Each reservoir is equipped with two sensors and the last one is located in the duct at the entrance of the nozzle.
- Each reservoir is suspended to a rigid structure via a strain gauge. The sensor elongation (function of the mass variation during the discharge) is converted into a voltage and then differentiated to obtain the total mass flow rate (Khir, 1987).
- Droplets velocity is measured with a laser Doppler velocimetry system (Jurski et al., 1996a,b).

4.1.2. Monodispersed aerosol generation

DOP particles are generated by an evaporation–condensation monodispersed aerosol generator as described by Liu et al. (1975). This generator (Fig. 3) provides a classical log-normal distribution defined by:

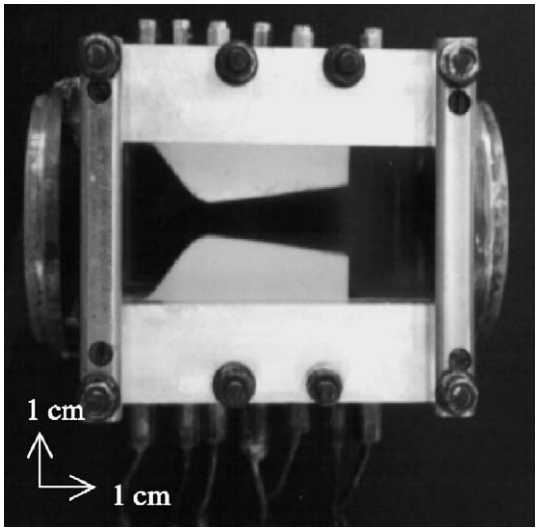

Fig. 2. View of the converging–diverging nozzle.

Table 1
Nozzle geometric characteristics

Converging length	28.5 mm	Rectangular entrance section	50×10 mm^2
Diverging length	47.5 mm	Square section at the throat	10×10 mm^2
Diverging angle	7°	Rectangular exit section	20×10 mm^2

Table 2
Ratio of the section in z to the throat section

$z(m)$	0.017	0.019	0.021	0.023	0.025	0.027	0.029
A/A_{th}	2.496	2.047	1.670	1.383	1.196	1.101	1.073

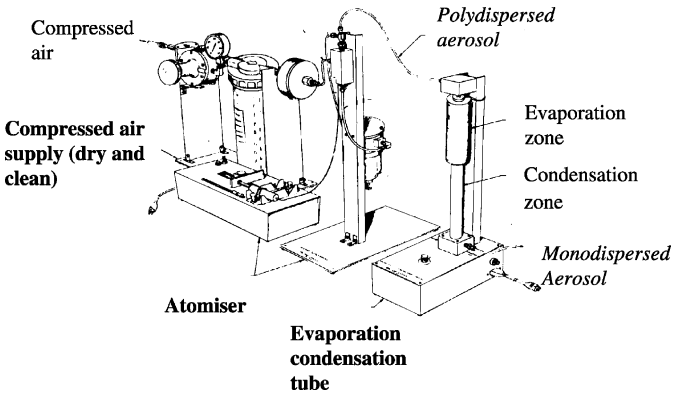

Fig. 3. Schematic representation of the evaporation–condensation monodispersed aerosol generator.

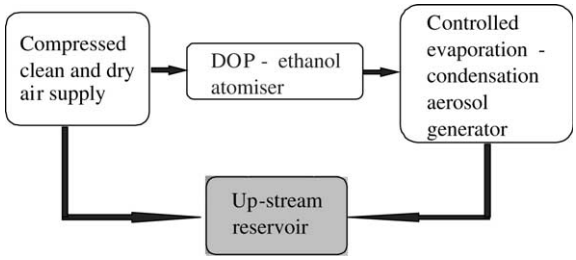

Fig. 4. Representation of the setup used in the seeding procedure of the upstream reservoir.

$$f(d) = \frac{1}{\log \sigma_g \cdot \sqrt{2\pi}} \cdot \exp\left[-\frac{(\log d - \log d_g)^2}{2\log(\sigma_g)^2} \right] \quad (1)$$

with d_g the median diameter and the geometric standard deviation $\sigma_g = 1.2$ (Renoux and Boulaud, 1998).

It involves a dry clean air supply system (TSI Inc. Model 3074), an impactor atomiser (TSI Inc. Model 3076) and an evaporation–condensation tube (TSI Inc. Model 3072) as proposed by Liu and Lee (1975). The DOP aerosol generation consists in two steps: polydispersed aerosol formation in the atomiser (DOP aerosol with a median diameter between 0.1 and 2 μm, with a volumic concentration higher than 10^7 p/cm^3) followed by a dispersion reduction around the required diameter in the evaporation–condensation tube.

4.1.3. Seeding procedure

The following seeding technique was used by Attoui et al. (1994). Generated DOP droplets are introduced in the upstream reservoir under ambient pressure conditions by means of a slow vertical downward circulation of dry and clean air exiting at the lower part of the reservoir. Thereby, the introduced aerosols tend to fill up the entire reservoir volume. This aerosol flow is

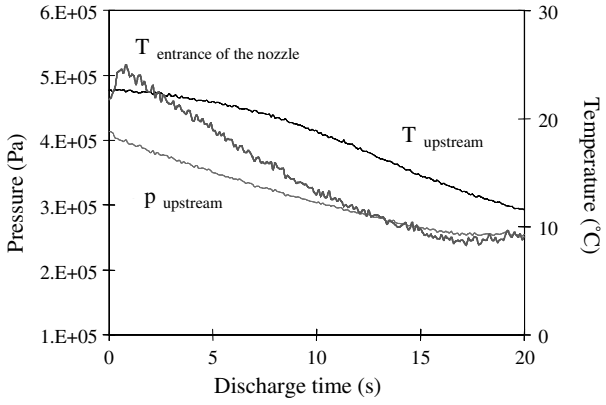

Fig. 5. Temperature evolution at the entrance of the nozzle, temperature and pressure evolution in the up-stream reservoir during the discharge.

periodically stopped in order to obtain a homogeneous concentration repartition in the reservoir (Fig. 4). The particles concentration is regularly controlled using a condensation nucleus counter (TSI model 3020) which allows particles concentration measurements up to 10^7 particles/cm^3 for diameters up to 1.3 μm.

Then, the upstream reservoir is slowly fed with clean wet air. The mixture humidity can be increased by adjunction of water before the pressure is increased.

4.2. Experimental flow characterisation

Typical initial pressure and temperature in the upstream reservoir are $p_{ui} = 4 \times 10^5$ Pa, $T_{ui} \sim 20$ °C and a 100% relative humidity (Fig. 5).

According to the low vapour proportion (2 g/kg of dry air), the mixture has the same pressure, temperature and mass flow rate characteristics as a single-phase fluid in equivalent flow condi-

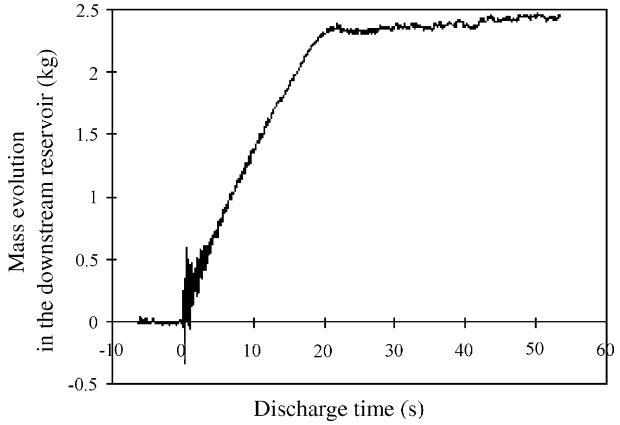

Fig. 6. Evolution of the mass transferred during the expansion from the upstream to the downstream reservoir.

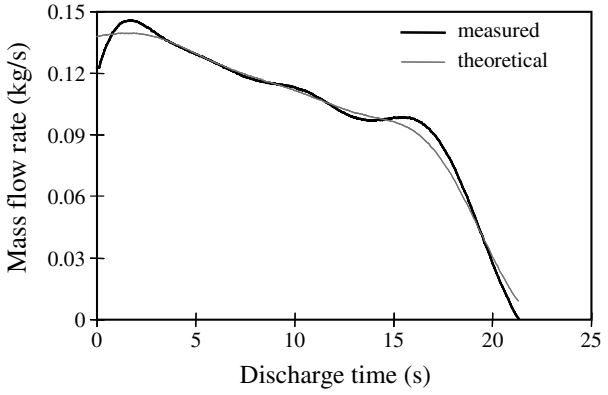

Fig. 7. Theoretical and measured evolutions of the mass flow rate.

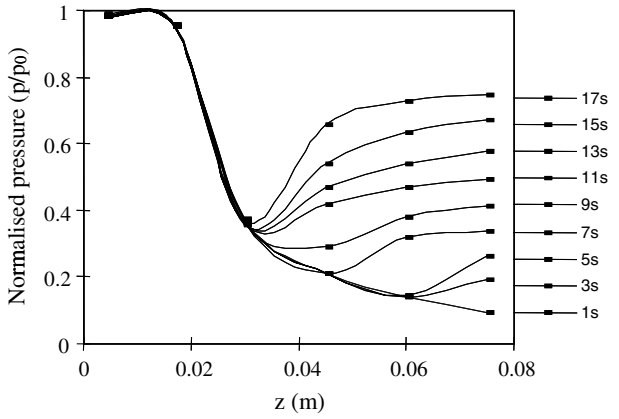

Fig. 8. Pressure profile in the nozzle as a function of time.

tions. Moreover, as suggested by Barrett and Baldwin (2000), the latent heat of condensation of vapour can be neglected. For an effective discharge of 20 s, the total mass transferred from the upstream to the downstream reservoir and the mass flow rate are given in Figs. 6 and 7 respectively.

The pressure profile measured in the nozzle during the discharge exhibits the following typical features for flow regimes in a nozzle (Fig. 8):

- Shock wave at the exit of the nozzle in the first seconds (sonic throat).
- Internal shock wave until $t = 15$ s (sonic throat).
- Generalisation of the subsonic regime in the entire nozzle after $t = 15$ s.

For clarity, Fig. 8 presents the pressure profile in $z(m)$ coordinates. The analogy of z with the section ratio is given in Table 2.

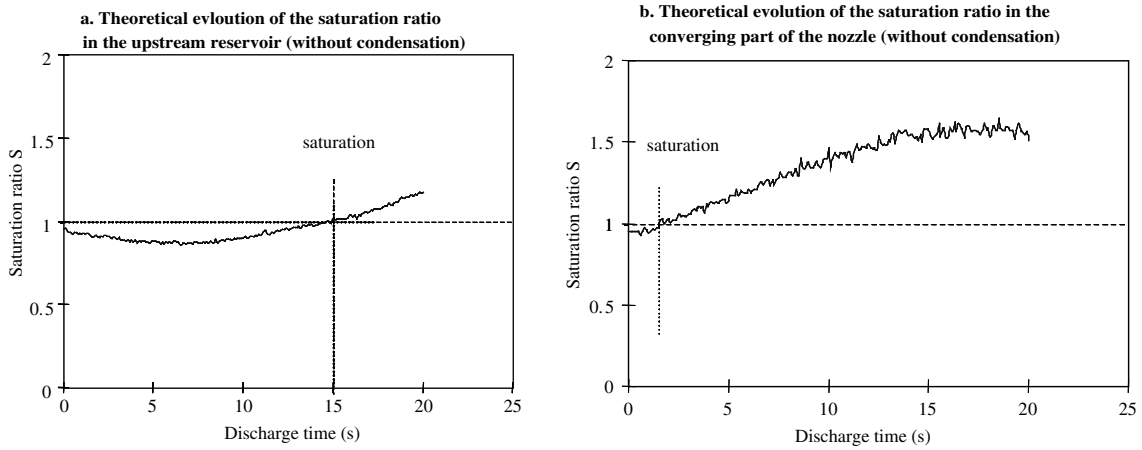

Fig. 9. Temporal evolution of saturation ratio S in the upstream reservoir and at the entrance of the nozzle. The displayed evolution is based on the assumption of absence of condensation process.

The saturation ratio required to initiate the condensation process ($S = 1$) is achieved in the nozzle at the beginning of the discharge and in the upstream reservoir at the end of the discharge (Fig. 9a,b).

5. Droplet velocity and diameter measurements

Several discharges series have been performed with a mixture of wet air and DOP nuclei of controlled concentration and diameter (0.4 or 1.3 μm diameter, and 10^4 or 10^7 p/cm^3 concentration, i.e. a DOP maximum mass of 9 g). Dop nuclei serve as condensation sites leading to water-coated DOP droplets. For each expansion, pressure, temperature and droplet velocities in the converging part of the nozzle have simultaneously been measured.

Notice that a previous study highlighted the fact that DOP aerosols of these diameters and concentration ranges in a dry clean air flow are not affected by coalescence and/or break up mechanisms during the transit time in the nozzle. They also exhibit good characteristics as seeding particles in our experimental conditions (Jurski et al., 1997; Jurski and Géhin, 1998).

5.1. Droplet velocity

As mentioned previously, the condensation process is:

- time-dependent since the vapour pressure varies for each location during the discharge time,
- depending on the location in the nozzle, since the vapour pressure decreases when reaching the throat.

For these reasons the time evolution and the spatial evolution of the measured velocity are needed.

Notice also that velocity measurements at a given location and time underlined a unique frequency peak, i.e. a unique characteristic velocity, leading to the assumption that all the droplets observed at this location and time have the same size (Jurski, 1997).

5.1.1. Time evolution

Fig. 10 displays gas and droplet velocity as functions of time at the middle of the converging part of the nozzle. This figure shows that the relative velocity (U_r) between gas and droplets rapidly increase in the first seconds of the discharge. Fig. 11a,b shows relative velocities U_r between the wet air and the droplets for different nucleus diameters and concentrations.

Relative velocities display four different stages of evolution:

- Absence of relative velocity between phases during the first seconds of the discharge (up to $t \approx 2$ s).
- Increase of U_r until $t = 4$ s (slope (a)).
- Slight increase (slope (b)) as long as the flow regime remains sonic ($t < 15$ s).
- Rapid decrease for $t \geqslant 15$ s, when the flow becomes subsonic in the entire nozzle (slope (c)).

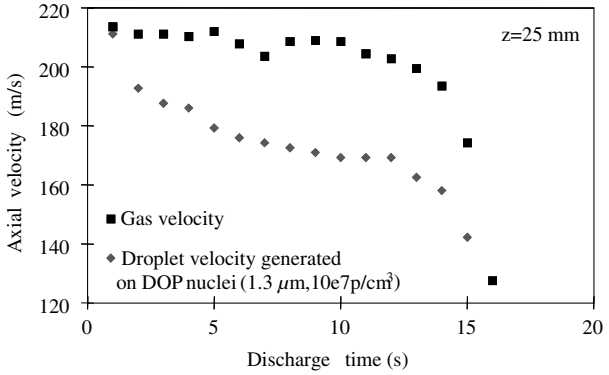

Fig. 10. Gas and droplet velocity as a function of time at the middle of the converging part of the nozzle.

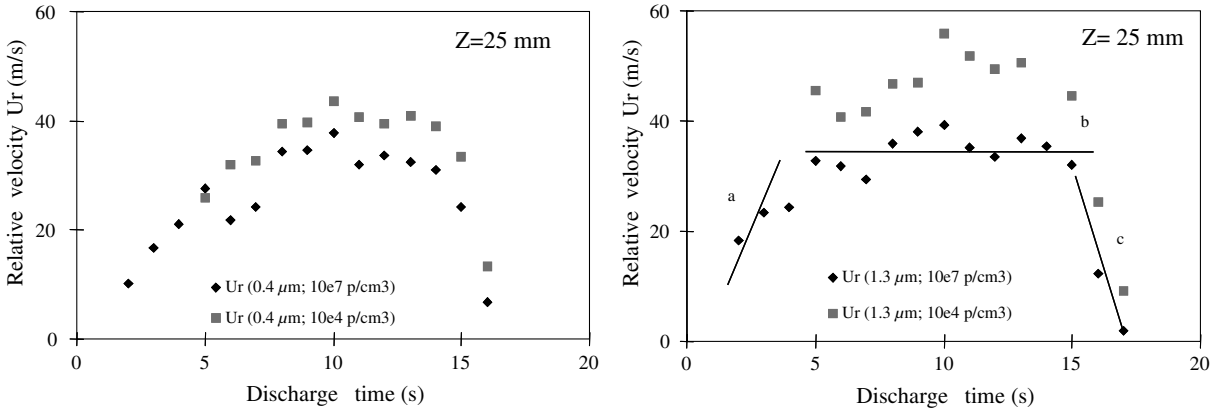

Fig. 11. Temporal evolution of relative velocities between gas and water droplets for different nuclei size and concentration highlighting three distinct slopes a, b and c (the shape is the same for different positions z in the converging part of the nozzle, not illustrated here).

The absence of relative velocity for $t < 2$ s is explained by the presence of a DOP aerosol and unsaturated wet air. The dispersed phase acts as seeding particles. After a few seconds, a saturation state is reached at the entrance of the nozzle (as shown previously in Fig. 9), promoting therefore the condensation of water vapour on the initial DOP aerosol (slope (a)). This later leads to some monodispersed DOP droplets coated with liquid water film (slope (b)).

The relative velocity evolutions depend upon the characteristics of the condensation nuclei. For a given nucleus diameter, the relative velocity between gas and droplets differ for different concentrations. For a given concentration with different nucleus diameters, the relative velocity evolutions are close for a 10^4 p/cm^3 concentration, and similar for a 10^7 p/cm^3 concentration. These experimental evidences show that a large number of initial DOP droplets leads to a higher velocity of coated droplets (because of their smaller size).

5.1.2. Spatial evolution

From a spatial point of view, Fig. 12 displays the velocity of gas and droplets generated on 1.3 μm DOP nuclei for different concentrations (10^4 and 10^7 p/cm^3) a few seconds after the beginning of the discharge ($t = 4$ s) in accordance with the previous remarks related to the condensation activation and the nuclei concentration influence.

5.2. Measured aerodynamic diameters

The diameters of the water droplets in the converging part of the nozzle have been determined using a method similar to the commercial systems of Aerodynamic Particle Sizer TSI type (Chen et al., 1990) based on the use of Eq. (2) and the relative inter-phase velocity measurements.

The water-coated DOP droplets grow significantly to exhibit an increasing relative velocity with the gas phase: accordingly, their aerodynamic flight characteristics change. Since no droplet deformation is expected for such geometric configuration and velocity range (Jurski, 1997), assuming that all droplets in a cross section have the same diameter, d_{ae} (the diameter of a sphere with density 1 g cm^{-3} having the same falling velocity as the considered particle) can be written via a drag coefficient and a momentum balance on droplets as:

$$d_{ae} = \frac{(3/4) \cdot C_D \cdot \rho_c \cdot U_r^2}{\rho_l \cdot U_l \cdot \frac{dU_l}{dz} + \frac{dp}{dz}} \tag{2}$$

With ρ_c and ρ_l the continuous phase and droplet density, U_r the relative velocity between gaz and droplets, U_l the droplet velocity and C_D the drag coefficient from Brauer and Mewes (1972):

$$C_D = 0.4 + \frac{4}{Re_l^{0.5}} + \frac{24}{Re_l} \tag{3}$$

where Re_l is the Reynolds number of droplets.

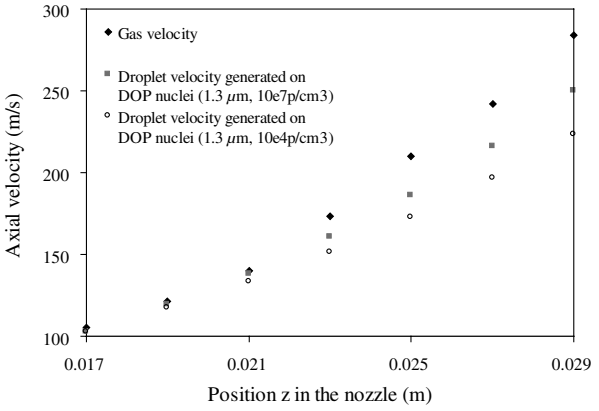

Fig. 12. Gas velocity and velocity of droplets generated on 1.3 μm DOP nuclei for different concentrations (10^4 and 10^7 p/cm^3) few seconds after the beginning of the discharge ($t = 4$ s).

Thus, under the same transport conditions, a relative velocity U_r between the phases determines a single aerodynamic diameter d_{ae}. This method leads to the determination of the aerodynamic mean diameter in the converging part of the nozzle for the different relative velocities displayed in Fig. 11a,b. d_{ae} has been determined for water droplets generated on 1.3 μm diameter DOP nuclei.

Figs. 13–15 show evolution of the droplet mean aerodynamic diameter in the nozzle at $t = 4$, 10 and 15 s after the beginning of the discharge. The droplet diameter increases as droplets flow from the entrance to the end of the converging part of the nozzle. Furthermore, the mean aerodynamic diameters are different for both nuclei concentrations (see Figs. 13–15). This difference increases with the discharge time (from $t = 4$ s to $t = 15$ s).

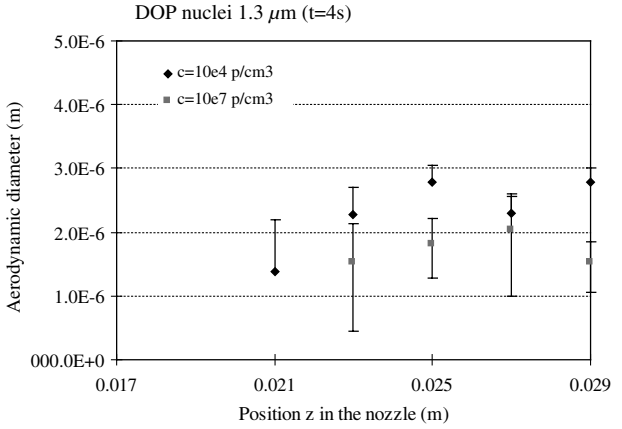

Fig. 13. Spatial evolution of the aerodynamic mean diameter of water droplets in the converging part of the nozzle at $t = 4$ s. d_{ae} has been determined for water droplets generated on 1.3 μm diameter DOP nuclei with different concentrations (10^4 and 10^7 p/cm^3). At $t = 4$ s, the upstream pressure is $p_{ui} = 3.6 \times 10^5$ Pa, the upstream temperature is $T_{ui} = 22$ °C and the temperature at the entrance of the nozzle $T_{z=0} = 20.5$ °C.

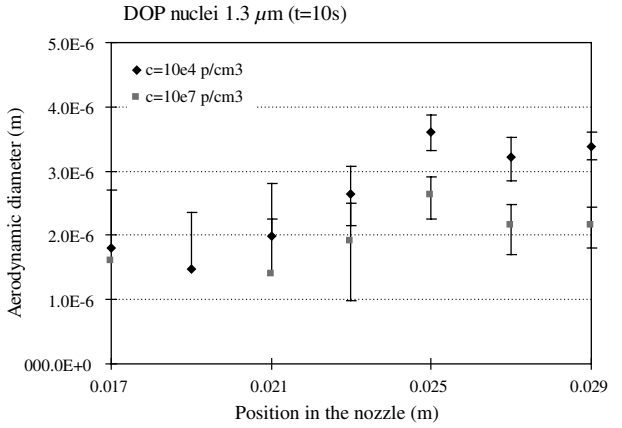

Fig. 14. Spatial evolution of the aerodynamic mean diameter of water droplets in the converging part of the nozzle at $t = 10$ s. d_{ae} has been determined for water droplets generated on 1.3 μm diameter DOP nuclei with different concentrations (10^4 and 10^7 p/cm^3). At $t = 10$ s, the upstream pressure is $p_{ui} = 3 \times 10^5$ Pa, the upstream temperature is $T_{ui} = 19$ °C and the temperature at the entrance of the nozzle $T_{z=0} = 13$ °C.

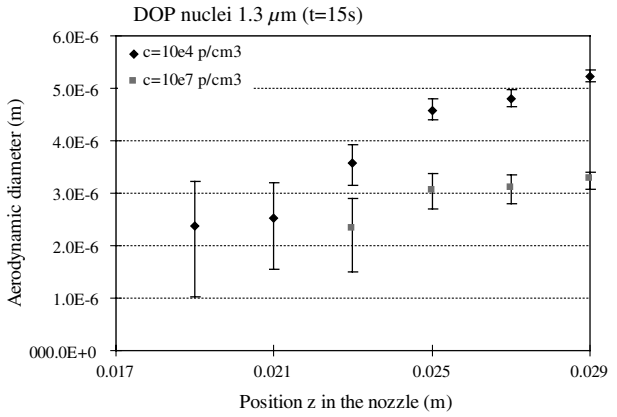

Fig. 15. Spatial evolution of the aerodynamic mean diameter of water droplets in the converging part of the nozzle at $t = 15$ s. d_{ae} has been determined for water droplets generated on 1.3 μm diameter DOP nuclei with different concentrations (10^4 and 10^7 p/cm^3). At $t = 15$ s, the upstream pressure is $p_{ui} = 2.8 \times 10^5$ Pa, the upstream temperature is $T_{ui} = 15$ °C and the temperature at the entrance of the nozzle $T_{z=0} = 9.5$ °C.

6. Conclusion

The purpose of this study was to highlight the influence of the diameter and concentration characteristics of impurities on the condensational process in a typical air and water unsaturated vapour expanding through a nozzle, where droplet formation and growth are governed by the vapour heterogeneous condensation on nuclei. Condensational growth of monodispersed DOP aerosols (0.4 and 1.3 μm diameters and concentrations ranging from 10^4 to 10^7 particles/cm^3) in a limited vapour source was studied to investigate the nuclei diameters and concentrations influence on the generated water droplets size.

The experimental results lead to conclude that the activation of water vapour condensation on the DOP nuclei is initiated as soon as the conditions of saturation are reached in the converging part of the nozzle, leading to monodispersed DOP droplets coated with a liquid water film. This set of experiments did not confirm the conjecture of Reist (1984) that condensation should proceed with more difficulty when the particles are not wettable. Such water-coated DOP droplets significantly grow to exhibit a large relative velocity with the gas phase in the nozzle. The aerodynamic mean droplet diameters determined on the basis of the particle aerodynamic flight characteristics, show both temporal and spatial growth of the water droplet diameter up to 5 μm from the entrance to the end of the converging part of the nozzle. In our experiments, the measured droplets' diameters, were shown to be affected by the initial particle concentrations.

The experimental results improved our understanding of the condensational process on particles and therefore should contribute to the modeling of such dispersed two-phase flows.

References

Amos, C.N., Schrock, V.E., 1984. Two-phase critical flow in slits. Nucl. Sci. Eng. 88, 261–274.

Attoui, M.B., Renoux, A., Vauge, C., Boulaud, D., 1994. Experimental and theoretical study of the filter efficiency at low pressure. IDOJARAS 98, 151–165.

Barrett, J.C., Baldwin, T.J., 2000. Aerosol nucleation and growth during laminar tube flow: maximum saturation and nucleation rates. J. Aerosol Sci. 6, 633–650.
Bayazitoglu, Y., Brotzen, F.R., Zhang, Y., 1996. Metal vapor condensation in a converging nozzle. Nanostruct. Mater. 7, 789–803.
Bird, R.B., Stewart, W.E., Lightfoot, E.N., 1960. Transport Phenomena. John Wiley & Sons, New York.
Brauer, H., Mewes, D., 1972. Chem. Ing. Technol. 44, 865–868.
Chen, B.T., Cheng, Y.S., Yeh, H.C., 1990. A study of density effect and droplet deformation in the TSI Aerodynamic Particle Sizer. Aerosol Sci. Technol. 12, 278–285.
Chexal, B., Horowitz, J., 1987. A critical flow model for flow through cracks and tubes. AIChE Symp. Ser., Heat Transfer 83, 218–222.
Chexal, B., Abdollahian, D., Norris, D., 1984. Analytical prediction of single phase and two phase flow through cracks in pipes and tubes. AIChE Symp. Ser., Heat Transfer 80, 19–23.
Cruz, C., Pandis, S.N., 1996. The effect of organic compounds on the ability of inorganic aerosols to become cloud condensation nuclei. AAAR'96, 11E3.
Fletcher, N.H., 1962. The Physics of Rainclouds. Cambridge University Press., p. 386.
Friedlander, S.K., 1977. Smoke, Dust and Haze, Fundamentals of Aerosol Behaviour. John Wiley & Sons.
Gorbunov, B., Hamilton, R., 1997. Water nucleation on aerosol particles containing both soluble and insoluble substances. J. Aerosol Sci. 28, 239–248.
Hidy, G.M., 1984. Aerosols, An Industrial and Environnement Science. Academic Press.
Hinds, W.C., 1982. Aerosol Technology, Properties, Behavior, and Measurement of Airborne Particles. John Wiley & Sons.
Hughmark, G.A., 1967. Mass and heat transfer from rigid spheres. Am. Inst. Chem. Eng. J. 13.
Johnston, M.V., Wexler, A.S., 1995. Mass spectrometry of individual aerosol particles. Anal. Chem. 67 (721A).
Jurski, K., 1997. Etude expérimentale du transport et de l'évolution granulométrique de gouttelettes microniques en écoulement critique en tuyère. Thèse de Doctorat, Université Paris XII—Val de Marne.
Jurski, K., Géhin, E., 1998. Splitting and coalescence criteria of droplets in a turbulent flow in a nozzle. J. Aerosol Sci. 29, S823–S824.
Jurski, K., Gehin, E., Piar, G., 1996a. Mesure de vitesses de gouttes dans un écoulement diphasique critique air—eau à faible teneur en eau par Anémométrie Laser Doppler, 5ème Congrès Francophone de Vélocimétrie Laser F3, 1–8, Rouen, France, 24–27 Septembre.
Jurski, K., Géhin, E., Degeratu, M., Piar, G., 1996b. Experimental study of a two-phase two-component critical flow in a converging–diverging nozzle. J. Aerosol Sci. (Suppl. 27), 419–420.
Jurski, K., Gehin E, Attoui, M.B., Piar, G., 1997. Comparaison des comportements d'aérosols de DOP et de gouttelettes d'eau en écoulement critique en tuyère convergente—divergente, Abstract du 12ème congrès Français sur les Aérosols. J. Aerosol Sci. 28, 1359.
Khir, T., 1987. Contribution à l'étude du retard à la condensation dans la détente d'une vapeur légèrement surchauffée d'une vapeur légèrement surchauffée d'un fluide frigorigène. Thèse de l'UniversitéParis XII—Val de Marne.
Kulmala, M., Vesala, T., Schwarz, J., Smolik, J., 1995. Mass transfer from a drop-II. Theoretical analysis of temperature dependent mass flux correlation. Int. J. Heat Mass Transfer 38, 1705–1708.
Lemonnier, H., Camelo Cavalcanti, S., 1993. Tailles et vitesses de gouttes àla sortie d'une tuyère parcourue par un écoulement diphasique à deux constituants, CENG/STI/LEF Grenoble, Société Française des Thermiciens, Journée d'études du 1èr Décembre 1993.
Lesniewski, T.K., Friedlander, S.K., 1997. Particle nucleation in turbulent gas jets. AIChE J. 43 (11A).
Liu, B.Y.H., Lee, K.W., 1975. An aerosol generator of high stability. J. Am. Hyg. Assoc. 36, 861–865.
Loyalka, S.K., Park, J.W., 1988. Aerosol growth by condensation: a generalization of Mason's formula. J. Colloid. Interface Sci. 125, 712–716.
Mallina, R.V., Wexler, A.S., 1997. Particle growth in high speed particle beam inlets. J. Aerosol Sci. 28, 223–238.
Mason, B.J., 1971. The Physics of Clouds, second ed Clarendon Press, Oxford.
Papon, P., Leblond, J., 1990. Thermodynamique desétats de la matière. Edition Hermann, Paris.
Rebours, A., Boulaud, D., Renoux, A., 1996. Recent advances in nanoparticles size measurement with a particle growth system combined with an optical particle counter—a feasibility study. J. Aerosol Sci. 27, 1227–1241.
Reist, P.C., 1984. Introduction to Aerosol Science. Collier MacMillan Publishers, London.

Renoux, A., Boulaud, D., 1998. Les Aérosols Physique et Métrologie. Lavoisier, Paris.
Sachweh, B.A., Büttner, H., Ebert, F., 1996. New technologies for the conditioning of waste gas to improve submicron particle separation by heterogeneous condensation of water vapor. AAAR'96, 6B1.
Selmer Olsen, S., 1991. Etude Théorique et expérimentale des écoulements diphasiques en tuyère convergente-divergente, Thèse de doctorat de l'Institut National Polytechnique de Grenoble.
Tom, J.W., Debenedetti, P.G., 1991. Particle formation with supercritical fluids. J. Aerosol Sci. 22, 555–584.
Turner, J.R., Kodas, T.T., Friedlander, S.K., 1988. Monodisperse particle production by vapor condensation in nozzles. J. Chem. Phys. 88, 457.
Vatazhin, A., Lebedev, A., Likhter, V., Shulgin, V., Sorokin, A., 1995. Turbulent air-steam jets with a condensed dispersed phase: theory, experiment, numerical modeling. J. Aerosol Sci. 26, 71–93.
Wegener, P.P., Pouring, A.A., 1964. Phys. Fluids 7, 352.
Wegener, P.P., 1969. Nonequilibrium flows, Part 1. Dekker, New York.
Wenqing, L., Jinfan, H., 1995. Phase and size control of nanometer-size materials synthesised in supersonic jet expansions. Mater. Sci. Eng. A 204, 205–210.
Williams, M.M.R., 1996. A model for the transport of vapour, gas and aerosol droplets through tubes and cracks. Prog. Nucl. Energy 30, 333–416.
Williams, M.M.R., Loyalka, S.K., 1991. Aerosol Science Theory and Practice—With Special Application to the Nuclear Industry. Pergamon Press, Oxford.
Wilson, C.T.R., 1927. On the cloud method of making visible ions and the tracks of ionizing particles. Nobel Lectures in Physics, 1922–1941.
Yang, J., Jaenicke, R., Dreiling, V., Peter, T., 2000. Rapid condensational growth of particles in the inlet of particle sizing instruments. J. Aerosol Sci. 31, 773–788.
Young, J.B., 1982. The spontaneous condensation of steam in supersonic nozzles. PhysicoChem. Hydrodyn. 3, 57–82.